Electronic Supplementary Material (ESI) for Nanoscale.

Supporting Information

Molybdenum Carbide and Oxycarbide from Carbon-Supported MoO_3 Nanosheets: Phase Evolution and DRM Catalytic Activity Assessed by TEM and *in situ* XANES/XRD Methods

Alexey Kurlov,[†] Xing Huang,*[,‡] Evgeniya B. Deeva,[†] Paula M. Abdala,[†] Alexey Fedorov,*[,†] Christoph R. Müller*[,†]

[†]ETH Zürich, Department of Mechanical and Process Engineering, Leonhardstrasse 21, CH 8092 Zürich, Switzerland

[‡]ETH Zürich, ScopeM, Otto-Stern-Weg 3, CH 8093, Zürich, Switzerland

E-mail:

* xing.huang@scopem.ethz.ch
* fedoroal@ethz.ch
* muelchri@ethz.ch

List of Figures

List of Tables

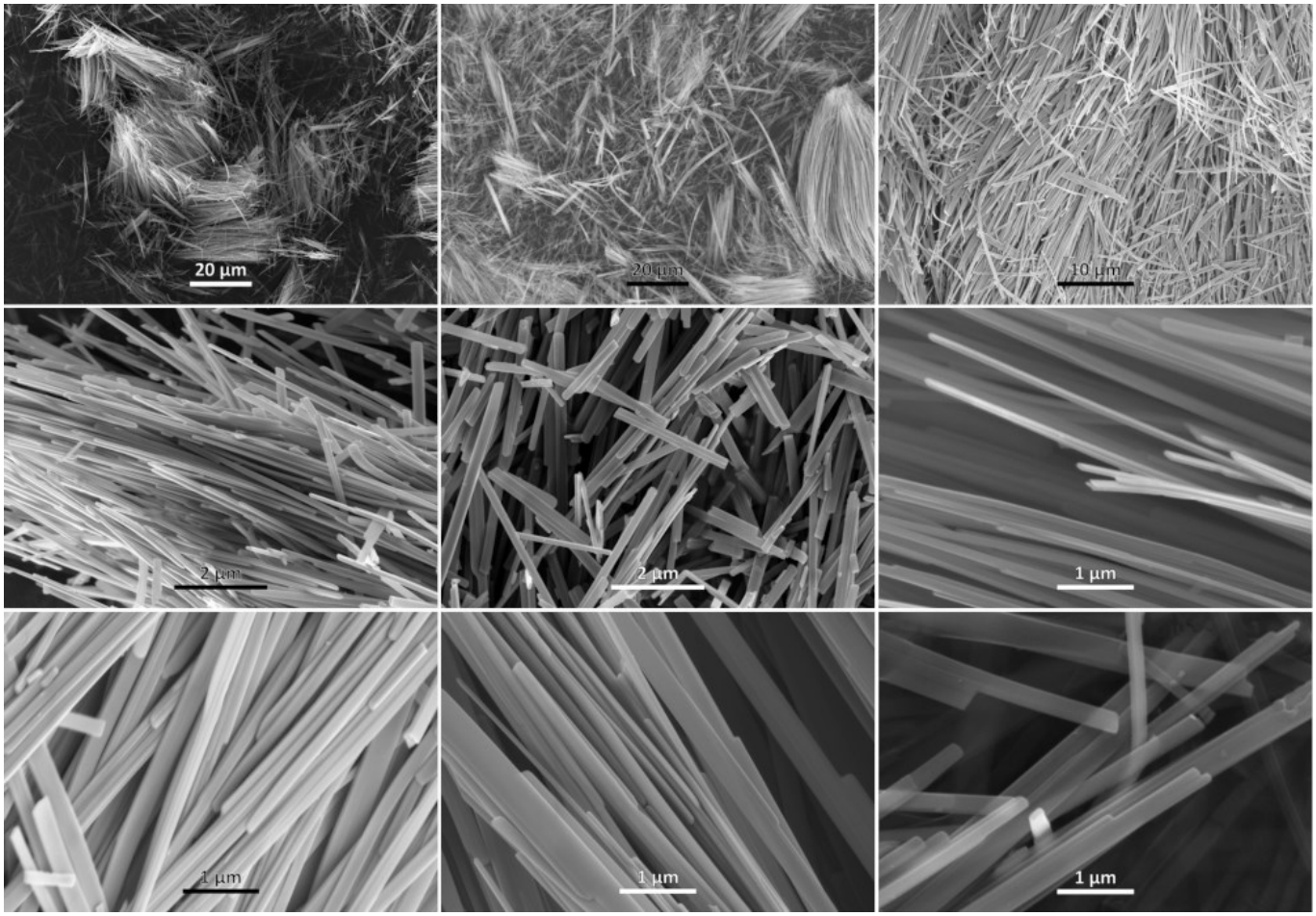

Figure S1. SEM images of α-MoO_3 nanobelts.

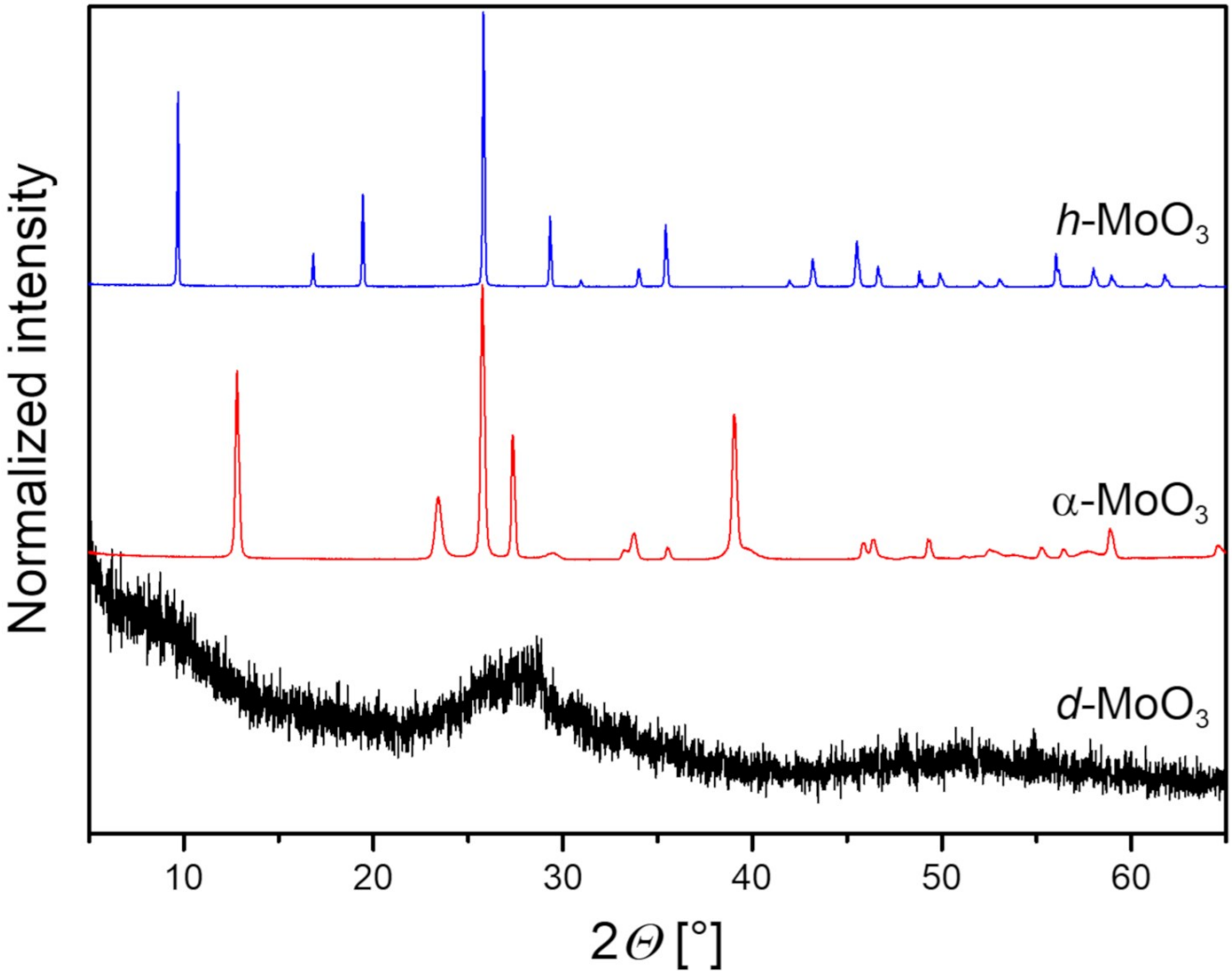

Figure S2. XRD (laboratory based) patterns of *h*-MoO_3, α-MoO_3 and *d*-MoO_3.

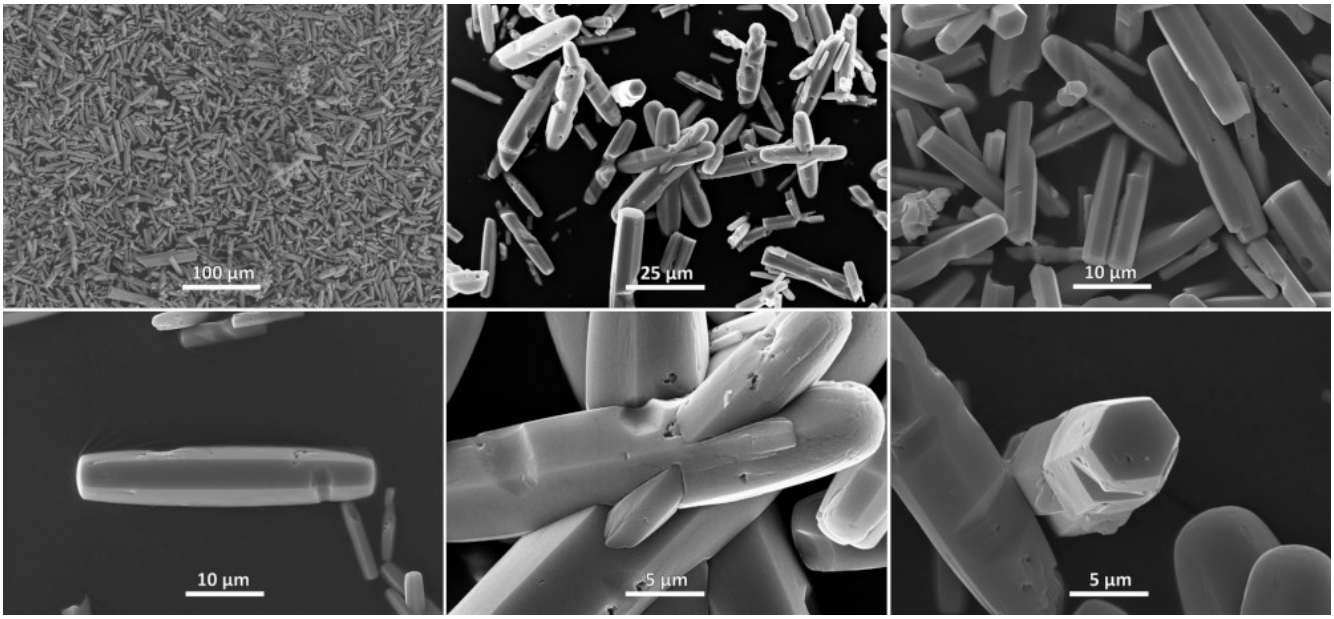

Figure S3. SEM images of *h*-MoO_3.

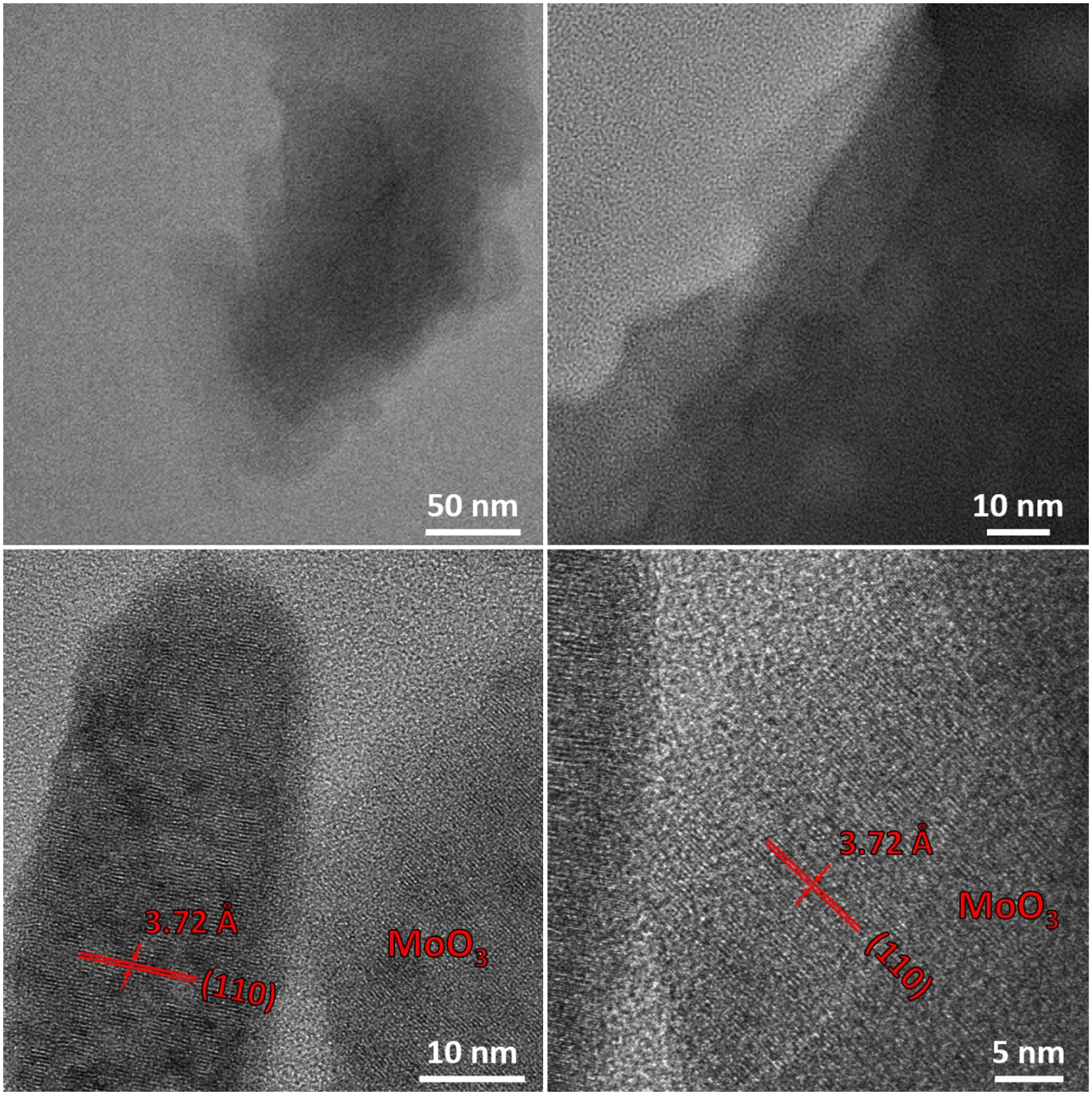

Figure S4. TEM images of exfoliated *d*-MoO_3.

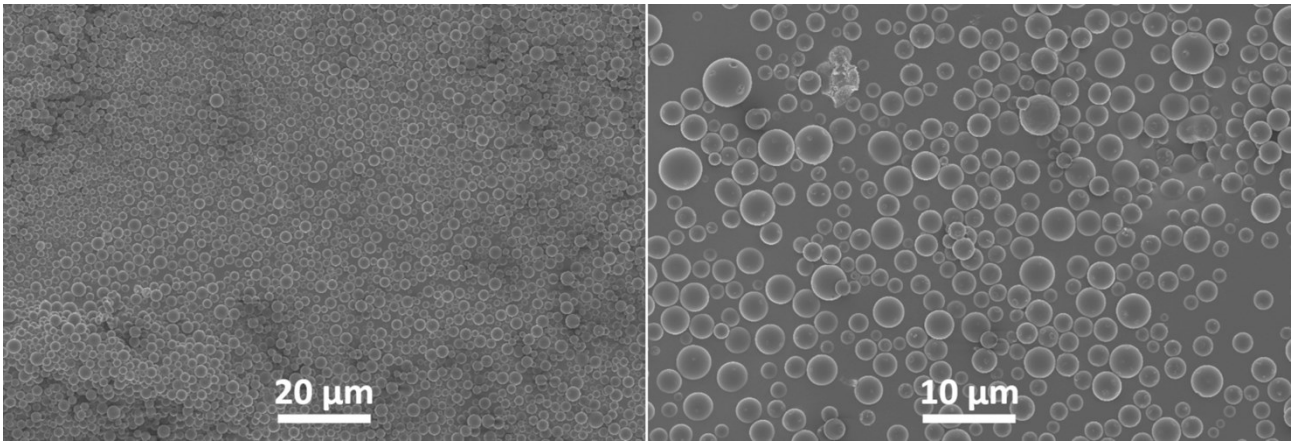

Figure S5. SEM images of carbon spheres.

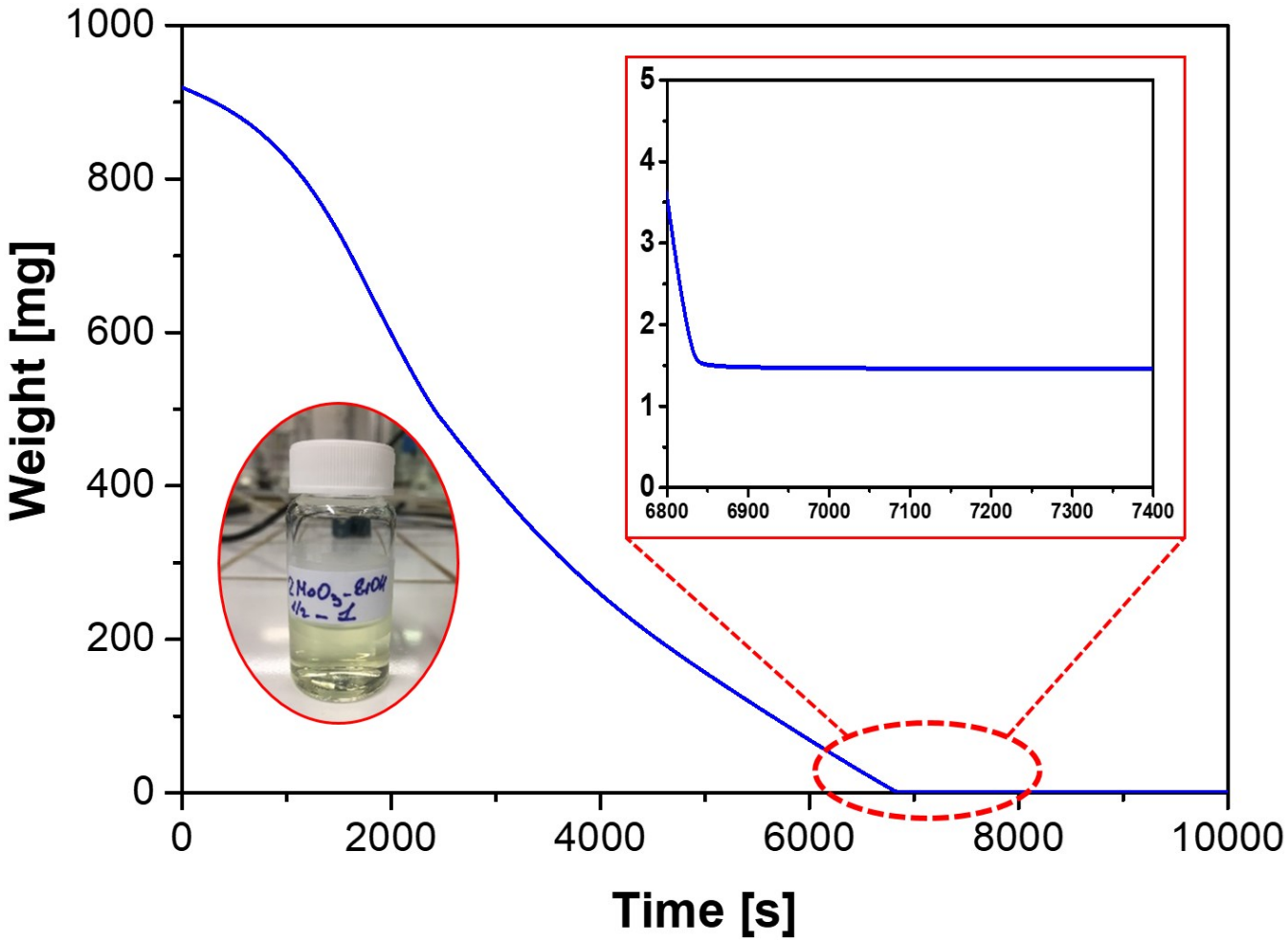

Figure S6. TGA weight loss curve of the *d*-MoO_3 colloidal solution.

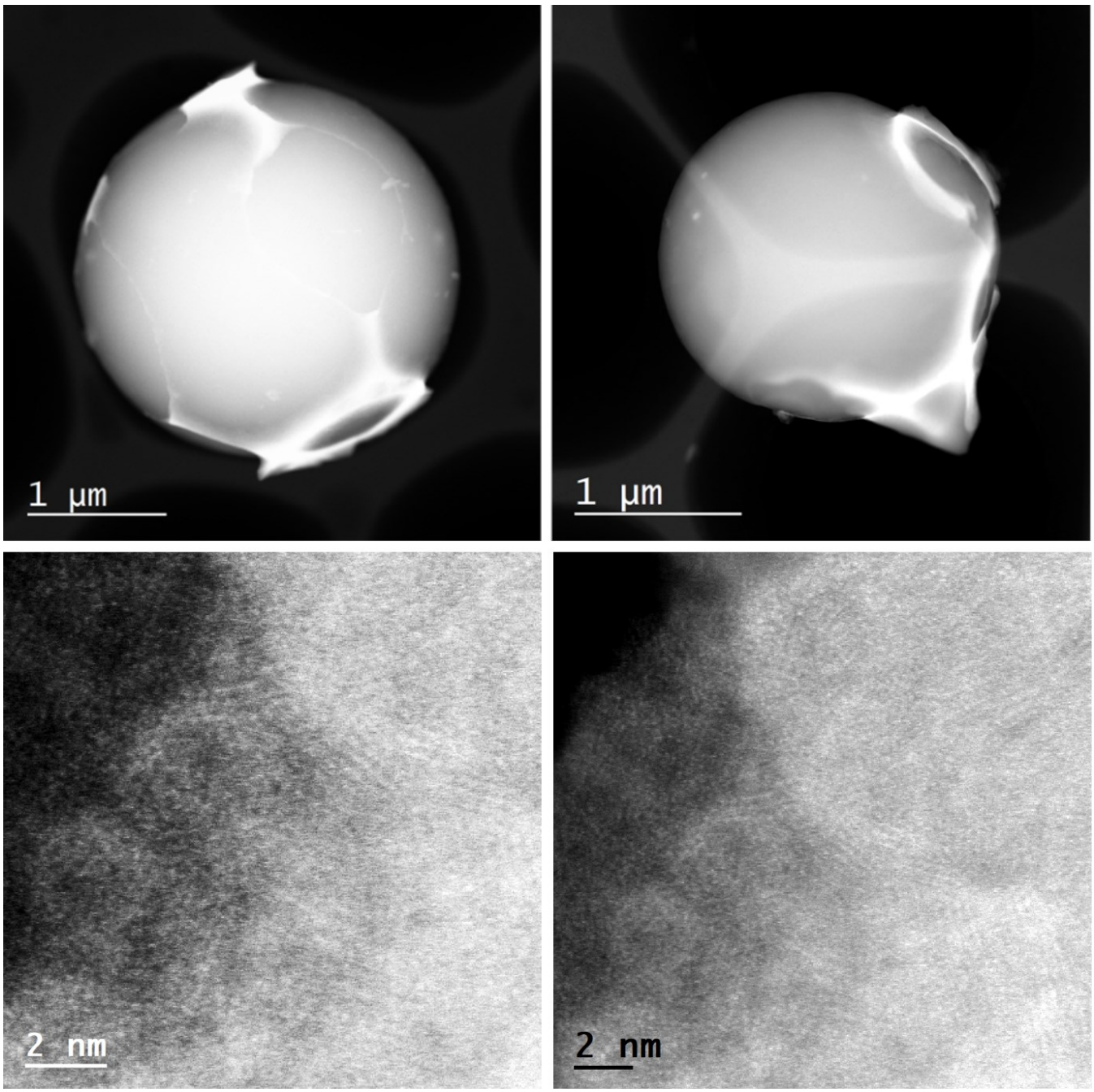

Figure S7. HAADF-STEM (top) and HR-STEM (bottom) images of *d*-MoO_3/C.

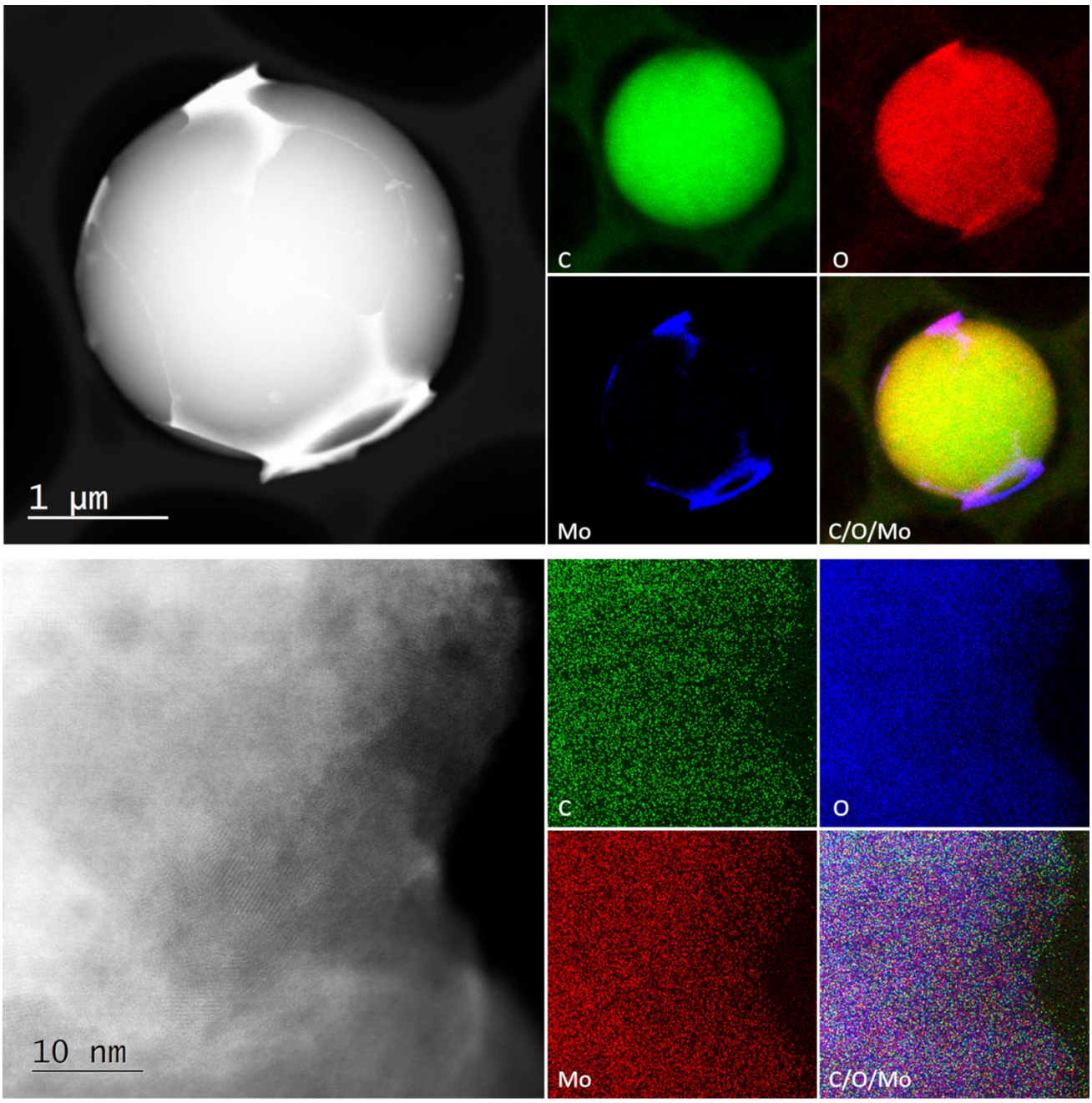

Figure S8. STEM/EDX mapping of *d*-MoO_3/C.

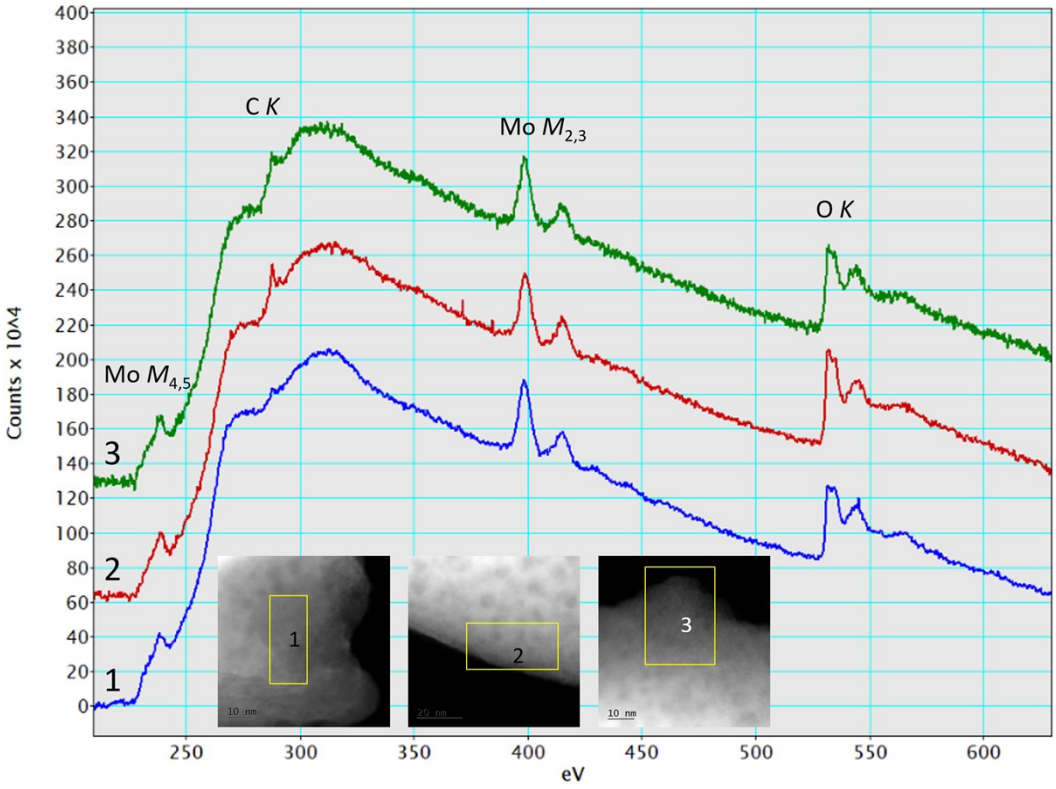

Figure S9. EELS spectra of the Mo-rich phase of *d*-MoO_3/C.

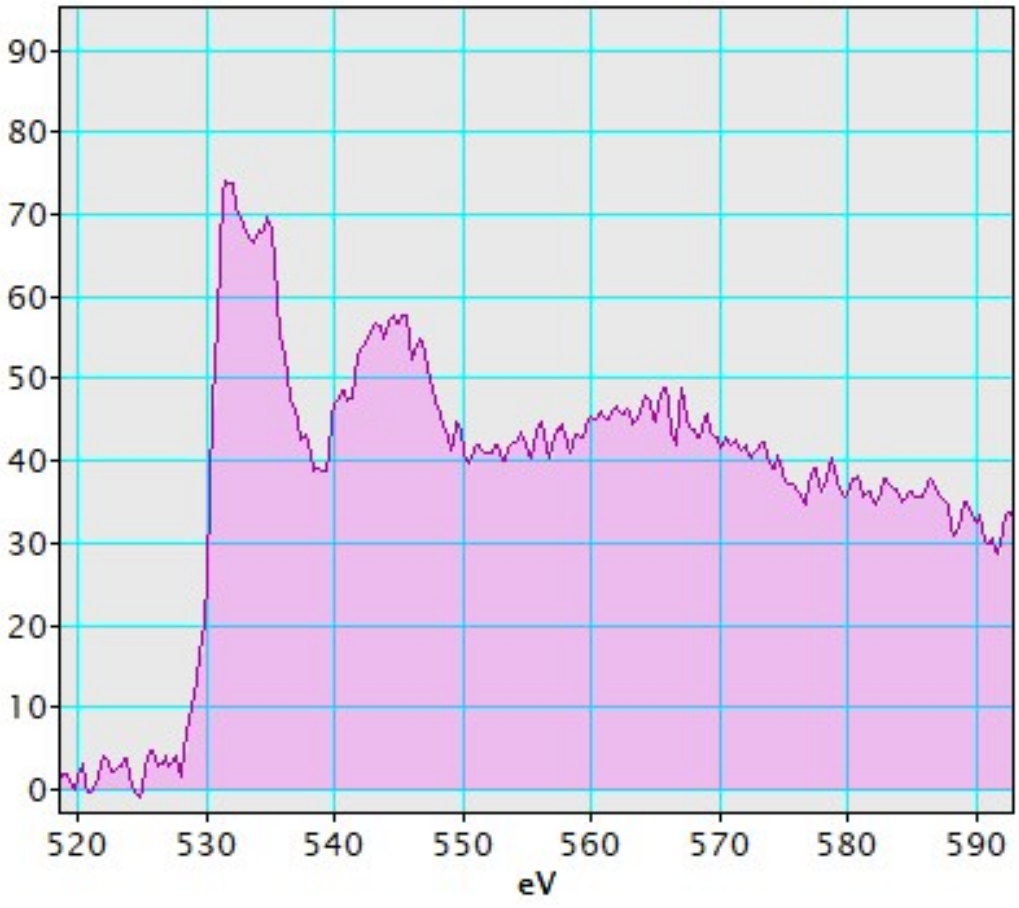

Figure S10. O K-edge spectrum of *d*-MoO_3/C.

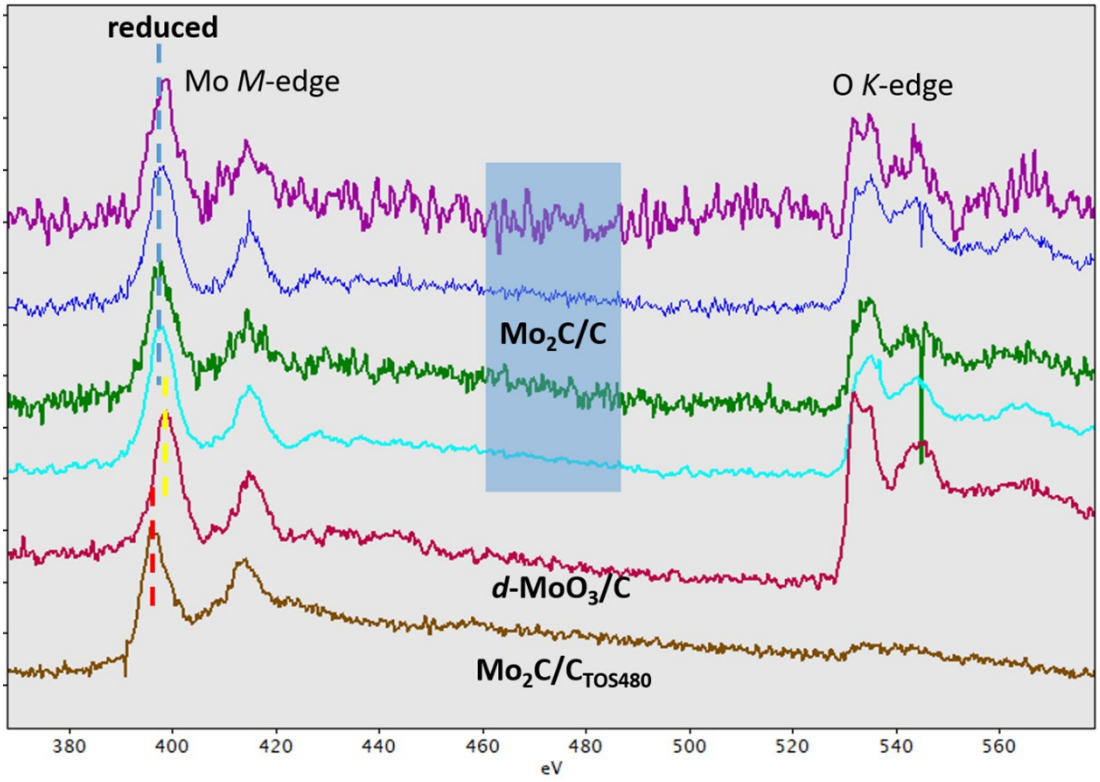

Figure S11. Comparison of EELS Mo $M_{2,3}$ edge and O K-edge of *d*-MoO_3/C, Mo_2C/C and Mo_2C/C_{TOS480}.

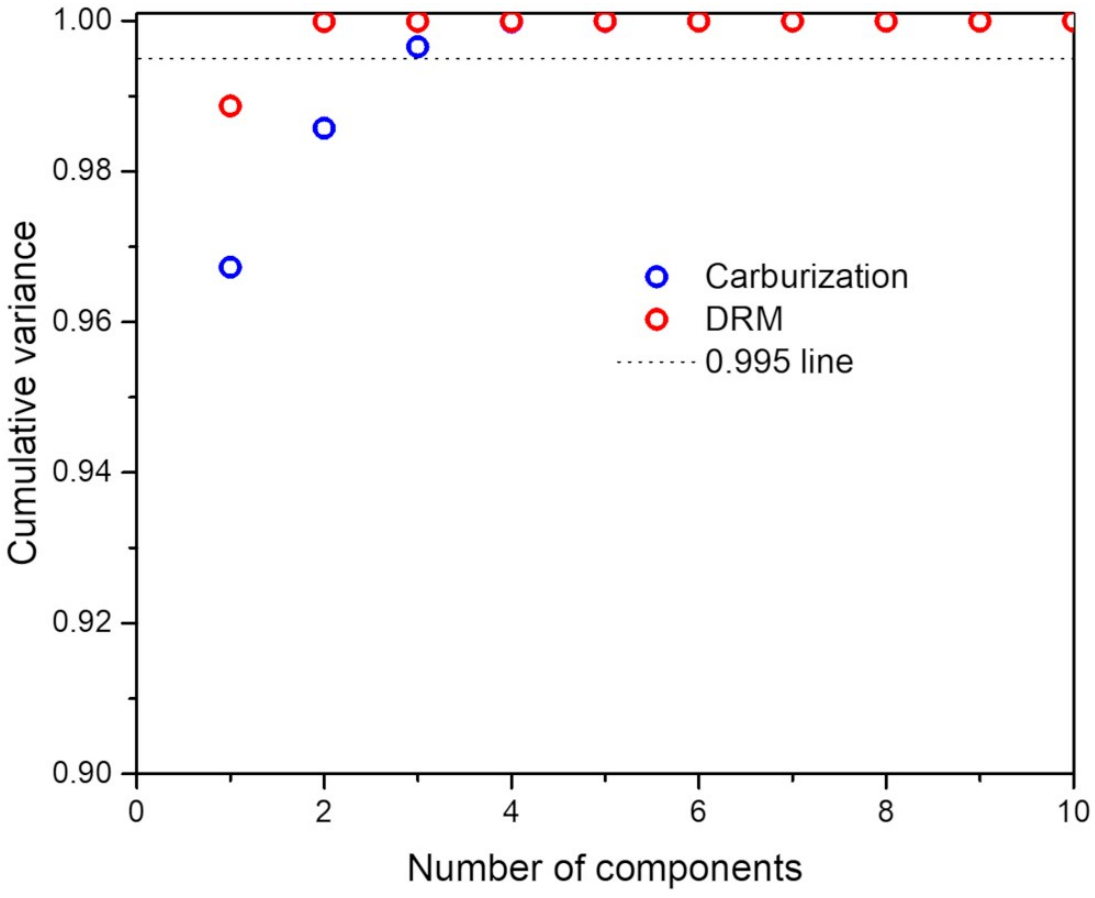

Figure S12. Cumulative variance plots obtained by principal component analysis (PCA) of the *in situ* XANES data during carburization and DRM.

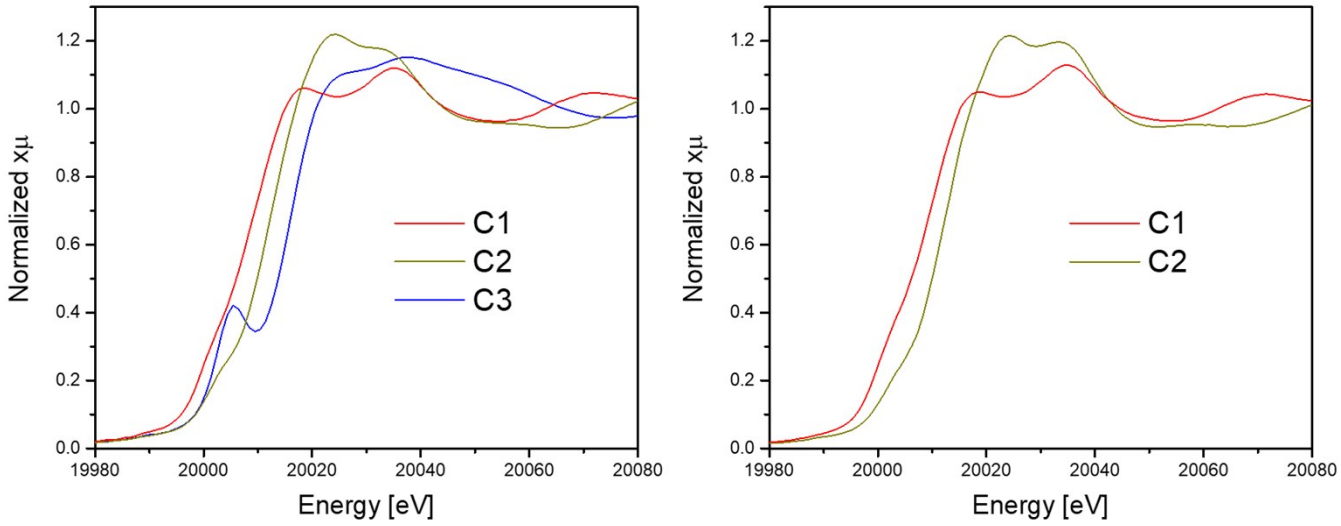

Figure S13. XANES spectra of the components obtained by MCR-ALS analysis during carburization (left) and DRM (right).

Table S1. Quality indicators of the MCR-ALS analysis of in situ XANES data obtained during the carburization and the DRM reaction.

Carburization	
Fitting error (lack of fit, LOF) in % (PCA)	1.4486×10^{-13}
Fitting error (lack of fit, LOF) in % (exp.)	0.45665
Percentage of variance explained at the optimum	99.9979
DRM	
Fitting error (lack of fit, LOF) in % (PCA)	1.9635×10^{-14}
Fitting error (lack of fit, LOF) in % (exp.)	0.35492
Percentage of variance explained at the optimum	99.9987

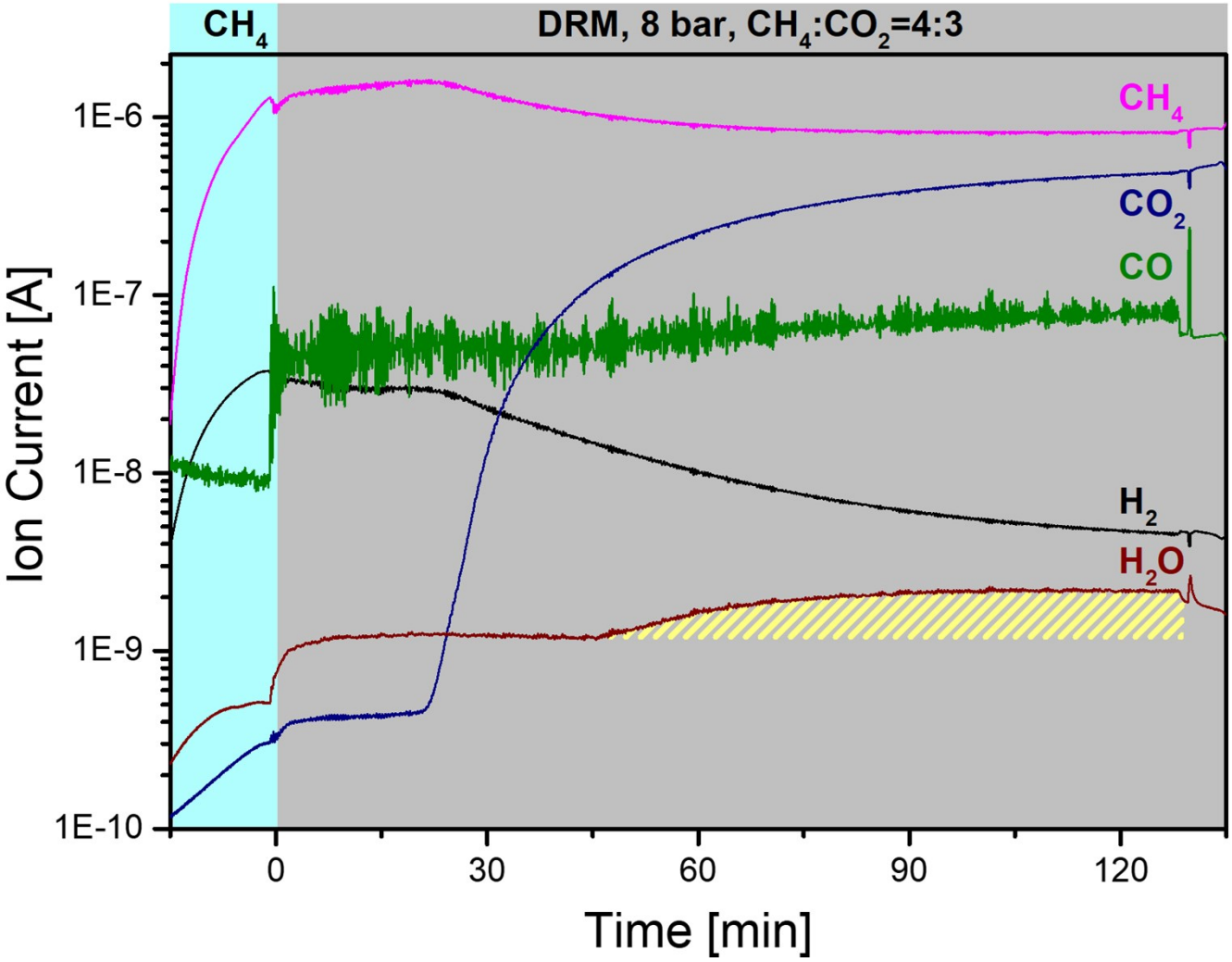

Figure S14. Trends in the composition of the off gas during the *in situ* DRM experiments as determined by a mass spectrometer (MS).

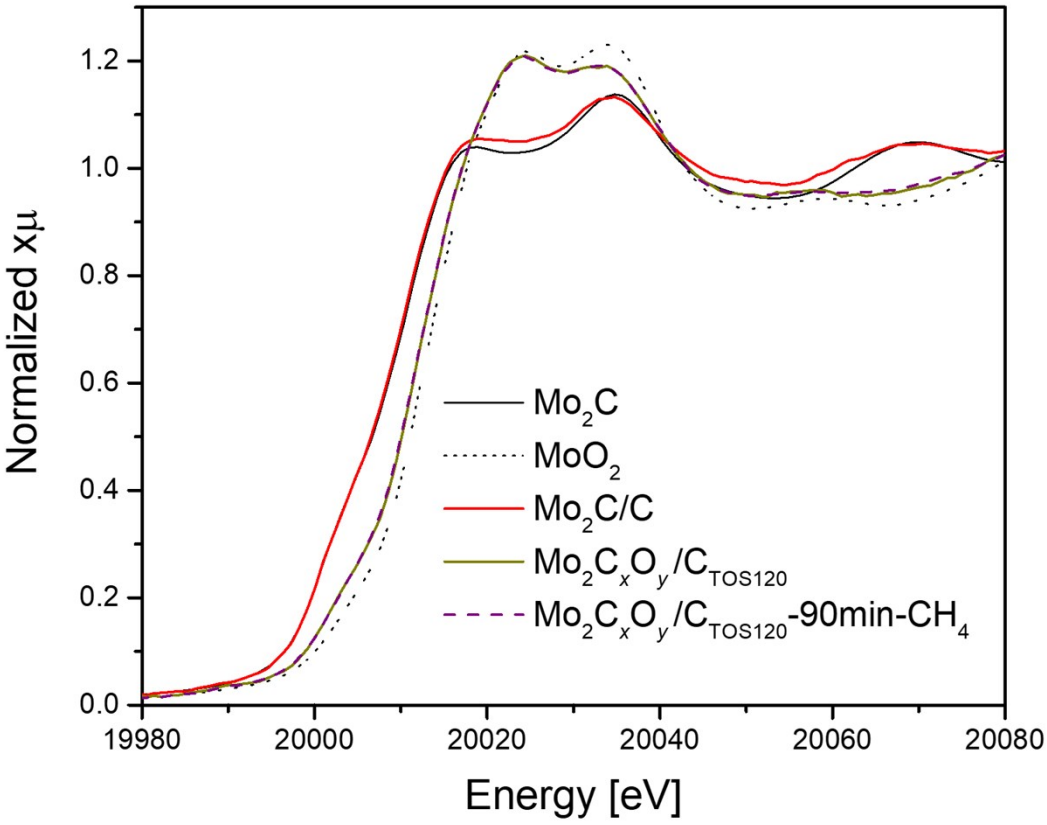

Figure S15. Comparison of the XANES spectra of the catalyst Mo_2C/C after having been exposed for 2 h under DRM conditions and after a re-carburization attempt in CH_4 for 90 min.

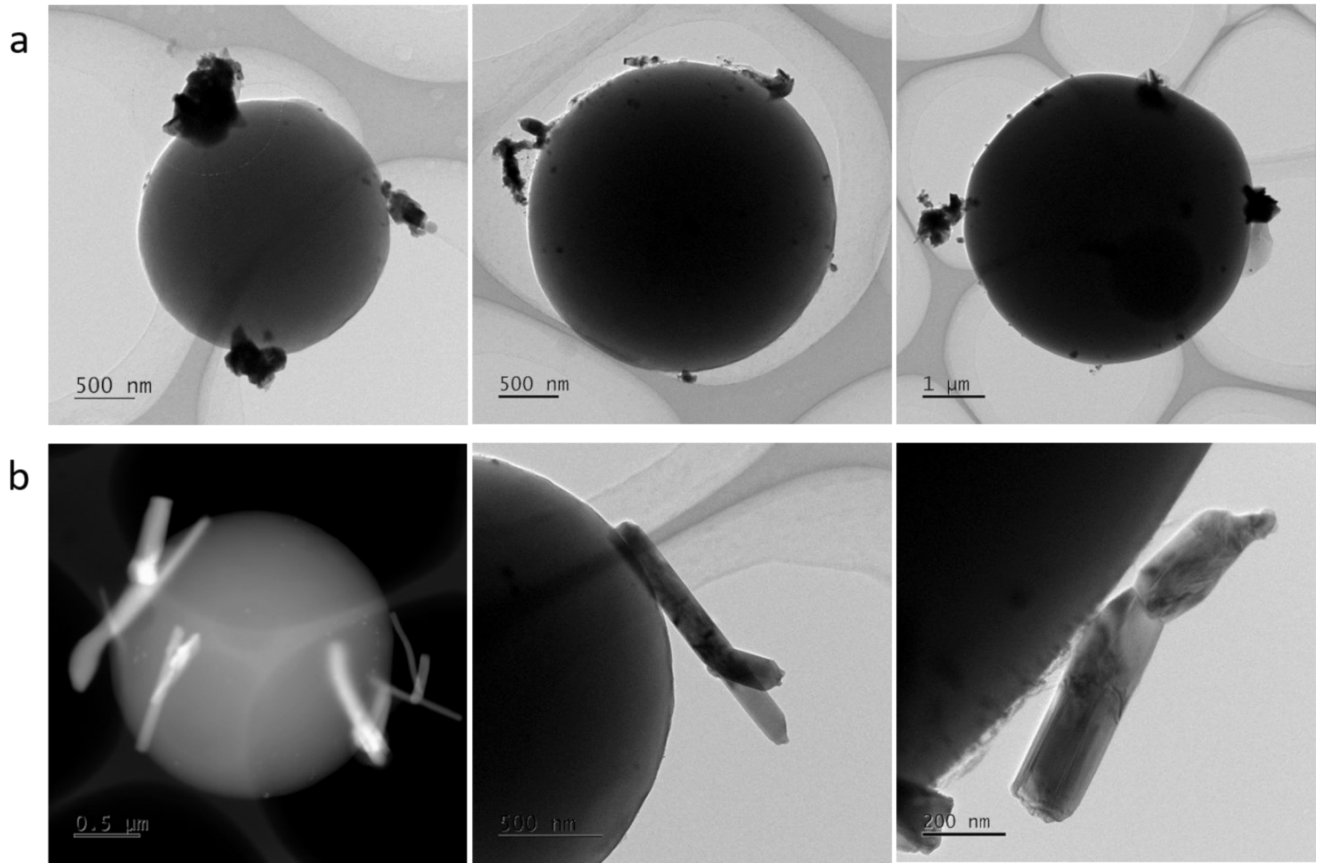

Figure S16. (S)TEM images of reacted $Mo_2C_xO_y/C$ with platelet (a) and nanorod (b) structures.

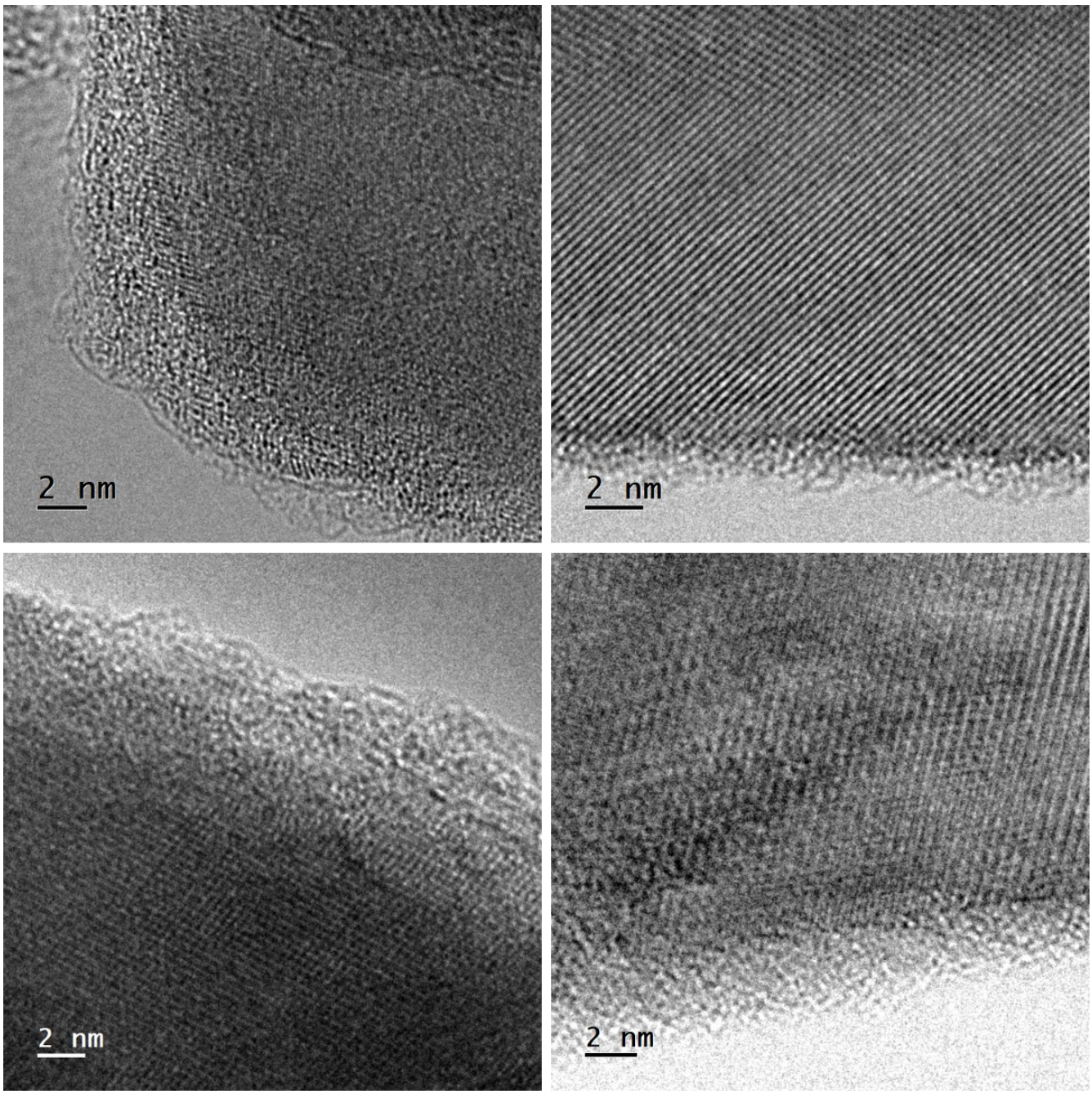

Figure S17. TEM images of reacted $Mo_2C_xO_y$/C indicating a surface layer with low crystallinity.

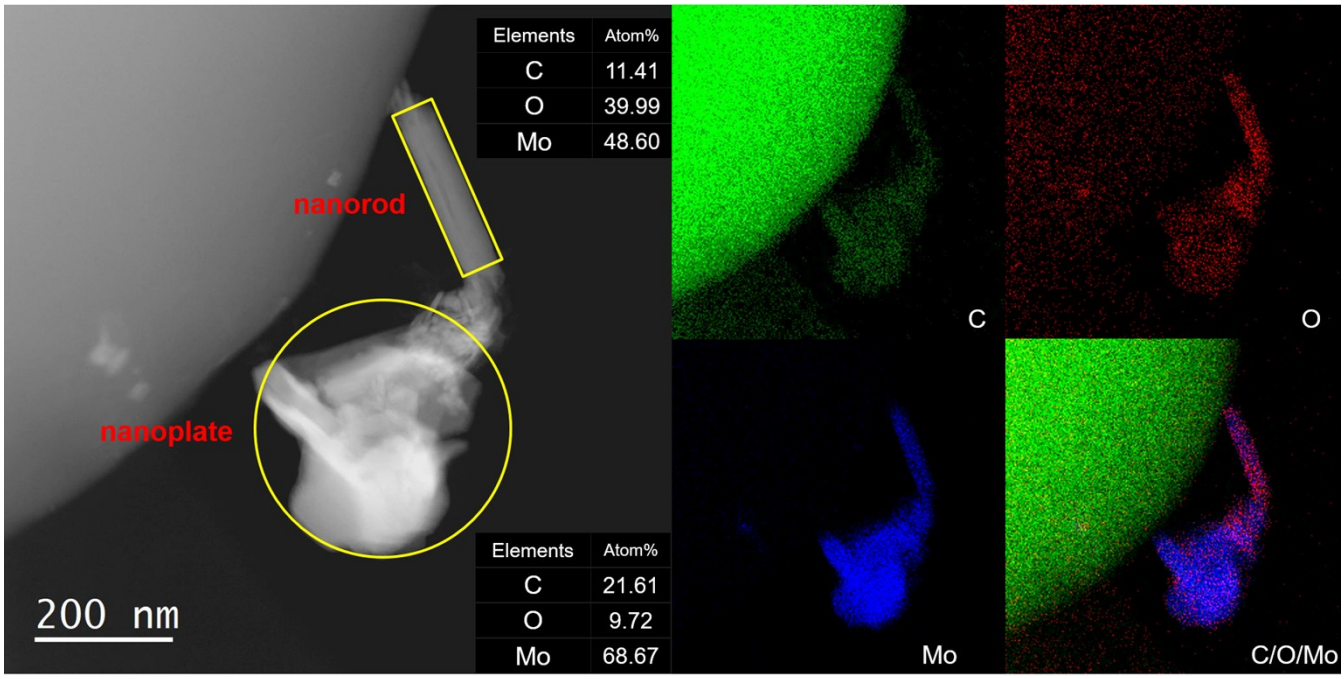

Figure S18. STEM/EDX mapping of reacted $Mo_2C_xO_y$/C indicating differences in the oxygen content in the various morphologies.

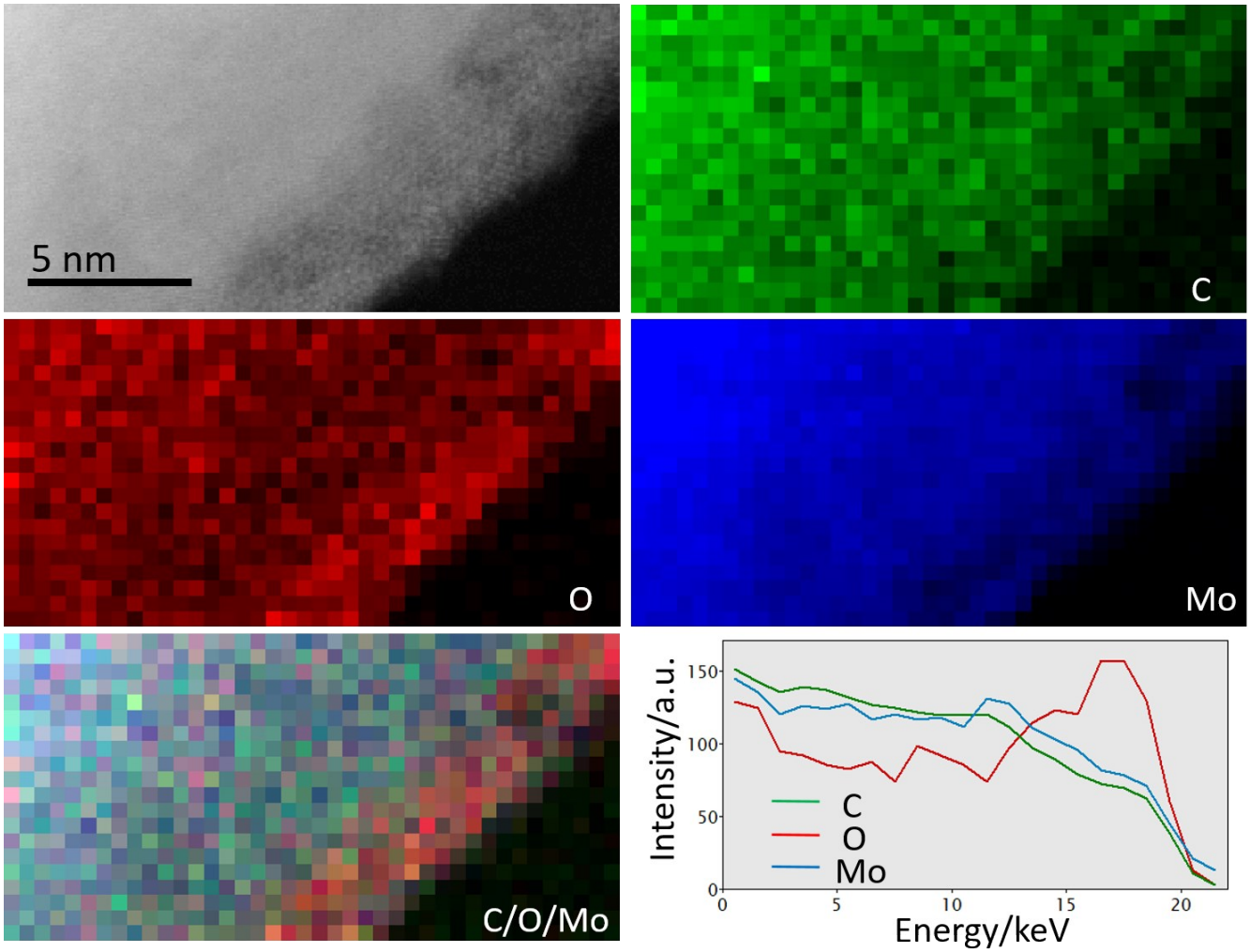

Figure S19. STEM/EDX mapping and EDX line profile of $Mo_2C_xO_y$/C indicating an O-rich surface layer.

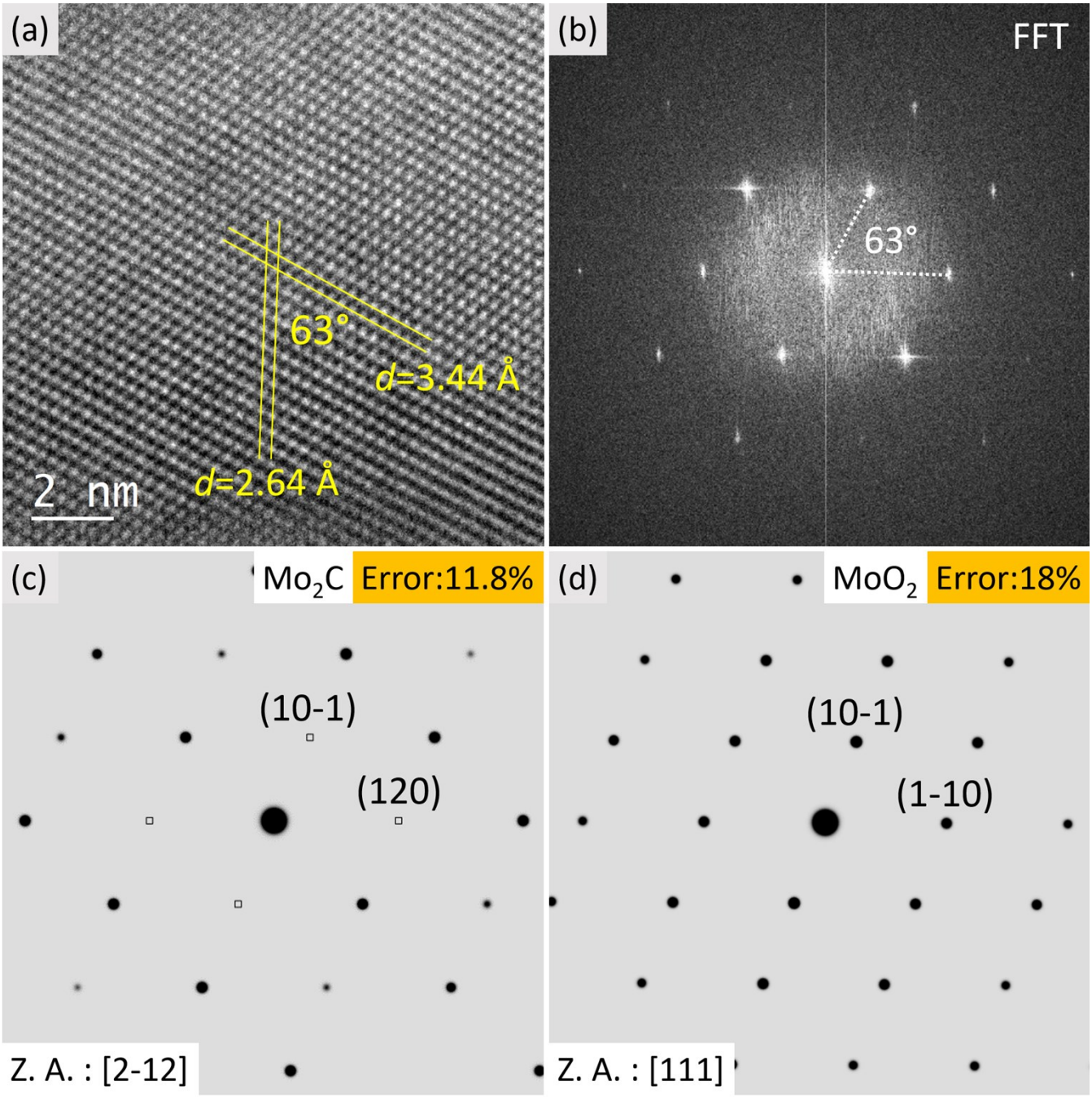

(e)

	(hkl)1	(hkl)2	d-hkl1	d-hkl2	Angle	Zone axis	Error
Mo_2C	10-1	120	3.51	2.54	66.74°	2-12	11.8 %
MoO_2	10-1	1-10	3.43	2.43	69.21°	111	18 %

Figure S20. a) HRTEM image of the $Mo_2C_xO_y$ nanorod in the spent catalyst and b) corresponding FFT; c), d) simulated electron diffraction along the most possible zone axis by referencing the standard Mo_2C and MoO_2; e) standard values calculated from the two reference structures; the errors are generated due to the misfit between our experimental data and the standard values.